NUCL SCI TECH (2018) 29:134
https://doi.org/10.1007/s41365-018-0462-5

Beam optics study for energy selection system of SC200 superconducting proton cyclotron

Xian-Hu Zeng[1,2] · Jin-Xing Zheng[1,2] · Yun-Tao Song[1,2] · Feng Jiang[1,2] · Ming Li[1,2] · Jun-Sheng Zhang[1,2] · Wu-Quan Zhang[1] · Lei Zhu[1]

Received: 10 October 2017 / Revised: 9 December 2017 / Accepted: 18 January 2018 / Published online: 30 July 2018

Abstract To meet the demands on proton therapy in Russia and China, JINR and ASIPP have started to develop a proton therapy facility based on an isochronous superconducting proton accelerator. A 200 MeV/500 nA proton beam will be extracted from the SC200 superconducting proton cyclotron. Due to the energy of the cyclotron being fixed, an energy selection system (ESS) is employed to degrade such energy in order to match the particle energy to a shallower depth. In this article, calculation of beam optics, analysis of beam transmission, and correction of orbit distortion are presented. Studies show that the main factors influencing transmission efficiency of the SC200 ESS beamline are the degrader, collimator, slit, vacuum system, beam diagnostic system, and trajectory correction system. Through the beam optics study, the designed ESS beamline can provide 70–200 MeV proton beam to a treatment room, with a maximum emittance of 24 π mm mrad. Also, the controllable momentum spread ranges from 0.1 to 1.0%, which is equivalent to an energy spread from 0.193 to 1.93%. The transmission efficiency about 0.204% can be obtained when the emittance is 24 π mm mrad with an energy spread of $\pm$ 0.6%.

This work was supported in part by the National Natural Science Foundation of China (No. 51507173) and Anhui Province Natural Science Foundation of China (No. 1608085QE93).

✉ Jin-Xing Zheng
jxzheng@ipp.ac.cn

1 Institute of Plasma Physics, Hefei Institutes of Physical Science, Chinese Academy of Sciences, Hefei 230031, China

2 University of Science and Technology of China, Hefei 230031, China

Keywords Proton therapy · Beam optics · ESS · Transmission efficiency · Orbit distortion correction

1 Introduction

Proton therapy has a unique advantage over traditional radiation therapy in that the proton beams deposit maximum energy at the end of their range, forming a sharp peak named the Bragg peak [1]. Proton therapy can significantly reduce side effects of healthy tissue surrounding tumors which has been accepted worldwide after successful patient treatments at Loma Linda University Medical Center [2]. To meet the demand of proton therapy in Russia and China, JINR and ASIPP started development of a proton therapy facility, modelled on a joint research centre operating in Hefei, China, since 2016, specializing in an isochronous superconducting proton accelerator [3]. The SC200 proton therapy facility mainly includes one superconducting cyclotron, one Gantry treatment room, and one fixed beam room. The main specifications are listed in Table 1.

However, when a (synchro) cyclotron was used to provide each treatment room with proton beams, one must take it into consideration that these machines would only operate with a fixed energy. It means that the maximum depth within the patient is determined by the fixed beam energy. In order to match the particle energy to a shallower depth, an energy selection system (ESS) must be employed to degrade particle energy and select the desired particle [4, 5].

The ESS is a special beam line, which works as a magnetic spectrometer with an energy degrader and a double-bend achromatic section. The beam energy is adjusted with a thickness-controllable wedge graphite

Table 1 Main specifications of SC00 proton therapy facility (PTF)

Parameters	Values
Beam energy of from the cyclotron (MeV)	200
Beam current (nA)	500
Emittance after cyclotron (π mm mrad)	≤ 5
ESS energy range (MeV)	70–200
Emittance after ESS (π mm mrad)	8–24
Gantry rotation angle (°)	± 185
Positioning precision at isocentre (mm)	≤ 1
FWHM at isocentre (in vacuum) (mm)	4–10
Delivery	PBS (downstream)
Field size (cm^2)	30 × 40

degrader. When the energy is selected, the energy spread is limited by the slit located in the middle plane of the double-bend achromatic beam transport system ($R_{16} = R_{26} = 0$). The passive energy-degrading method brings about a significant increase in energy spread due to multiple scatterings inside the graphite block. Therefore, each beam with different energy has different beam optical parameters. A collimation system should be installed next to degrader to optimize the beam properties so as to meet the demands of clinical treatments. In this paper, an investigation of ESS for SC200 proton therapy facility is presented. And the study is divided into several sections including beam optics, analysis of transmission efficiency, and orbit distortion correction.

2 Experimental section

2.1 Overall consideration for ESS

The basic element of beam optics is the achromatic beam transport, which is independent of the beam energy spread. Wherever possible, the beam transport system consists of symmetrical optical components which reduce the occurrence of optical aberrations and phase space dependence and minimize the effects of small errors in the settings of beamline components. The layout of ESS, shown in Fig. 1, is designed based on the calculation of beam optics, which consists of a fixed-energy beamline (FEB), an energy degrader, two collimators, and a double-bend achromatic beam transport system with an energy selection slit. The FEB is situated next to the cyclotron and composed of four quadrupoles (QC1–QC4) with a total length of 5.2 m. The energy degrader consists of two multi-wedge graphite blocks aimed at the energy modulation through adjusting its thickness. Two collimators (COL1 and COL2) are used to control the beam emittance. A

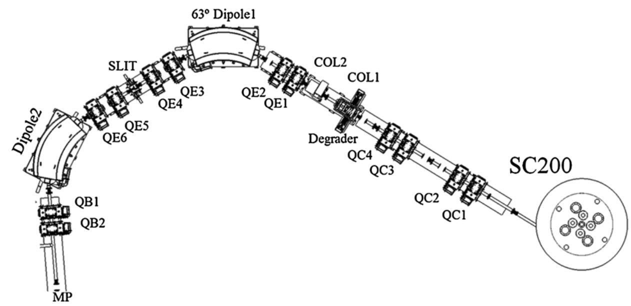

Fig. 1 Schematic layout of SC200 ESS (steering magnets and BPMs are hidden)

double-bend achromatic beam transport system consists of two dipoles (Dipole1 and Dipole2, each bending the beam over typically 45°–65°), eight quadrupoles (QE1–QB2), and a slit, which is located behind the collimator system. And the main optics considerations about ESS are summarized as follows:

- An energy degrader with two multi-wedge blocks placed opposite to each other is positioned just behind FEB.
- An energy analysis system is placed behind the degrader, which includes a symmetrical double-bend achromatic section with a size-changeable energy slit.
- At the matching point (MP), mirror and symmetrical round beam ($x = y$, $x' = y'$) is designed to match with beam transfer line.
- For verification of the optics and correcting orbit distortion along the ESS, a series of beam monitors for both directions (in x and y) and steering magnets are required.

2.2 Beam optics design

Figure 2 shows the first-order transport envelopes between the cyclotron reference point and matching point (MP). The optical design for ESS is divided into two different sections.

- Cyclotron reference point to degrader (fixed-energy beamline)
- Degrader to matching point (EAS)

These are discussed in more detail in the following section.

2.3 Fixed-energy beamline (FEB)

The results of TRANSPORT [6] calculations done for the fixed-energy beamline are shown in Fig. 2. The accelerator and degrader are connected with four quadrupoles (QC1–QC4) behind the cyclotron. Such a design can

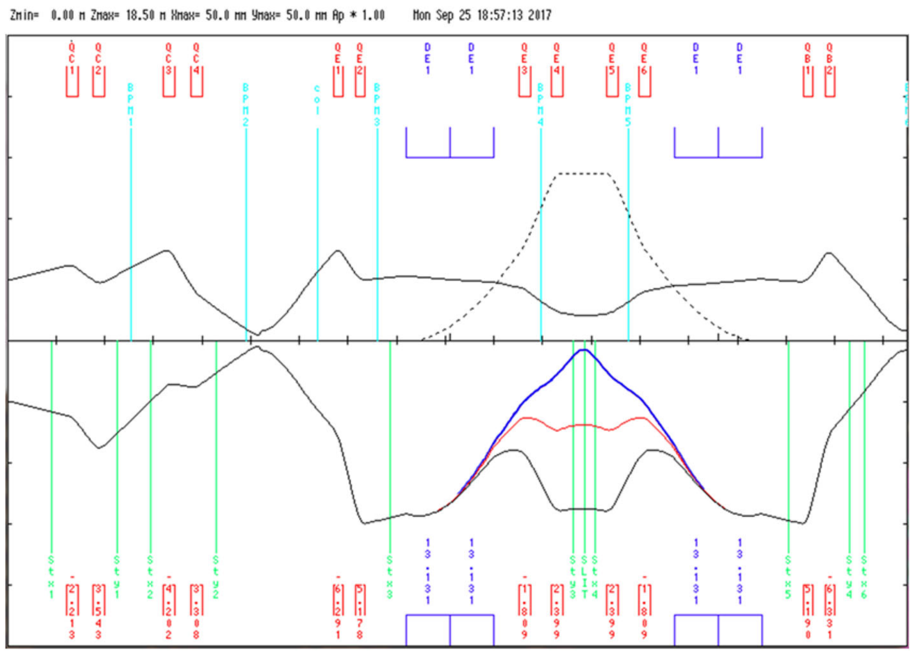

Fig. 2 Beam optics in the ESS. The half beam size is plotted as a function of the position along the beamline. Above the x-axis, the vertical beam size is plotted as a solid line and the 1%-dispersion trajectory as a dashed line. Below the x-axis, the horizontal beam size is plotted. And at the dispersive focus, both envelopes for dp/p = 0, 0.5 and 1% are drawn with blue, red and black lines (Color figure online)

create more flexibility for a proton beam extracted from the cyclotron to focus on the centre of the degrader compared with a Q-triplet. At the same time, it is better to form as a small round beam spot about 1–2 mm as possible, to improve the transmission efficiency.

2.4 Energy analysis system

Behind the fixed-energy beamline, a wedge graphite energy degrader is used to decrease the fixed-energy proton beam to any value in the range of 70–200 MeV. Due to multiple scattering in the degrader material, beam divergence and beam size increase towards the exit of the degrader when the exit energy decreases. A collimation system for emittance matching is designed to limit the emittance of the beam leaving the degrader whose emittance can be calculated with Eq. (1).

$$\varepsilon = 2R_1R_2/L, \tag{1}$$

where R_1 is the radius of the entrance collimator, R_2 is the radius of the exiting collimator, L is the total length between two collimators, and the emittance definition of Eq. (1) is valid only when the alpha parameters are zero. The first collimator immediately following the degrader is used to control the beam size, and the second collimator at a distance of approximately 1–1.5 m behind the degrader is used to control the beam divergence. Phase space is shown in Fig. 3.

After the collimator, the proton beam is focused using one focusing and one defocusing quadrupole, guided into the double-bend achromatic section. It is better to design a small vertical beam envelope or a vertical beam waist lactating in the bending magnet as much as possible, so that a gap size of 60 mm is sufficient. The first bending magnet will create a large horizontal dispersion to the beam which will be enlarged using a subsequent horizontal defocusing quadrupole. The dispersion will then reach a maximum value using a focusing horizontal quadrupole, which will remain unchanged in the drift space because the derivative of dispersion is zero ($R_{26} = 0$).

For a beam with a different momentum spread, the beam will be spread out across the horizontal plane. A correlation exists between the momentum of the protons and their distance to the centre trajectory, as shown in Fig. 4.

Therefore, a horizontal slit is set in the middle of the two horizontal focusing quadrupoles to select the required energy for clinical therapy by adjusting its aperture. The half-aperture of the slit for a different momentum spread can be calculated with Eq. (2).

$$\sigma_x = \sigma_{x0} + \delta^2 R_{16}^2, \tag{2}$$

where $\sqrt{\sigma_x}$ is the half envelope of beam and $\sqrt{\sigma_{x0}}$ is the half envelope of beam located at the slit depending on the beam itself regardless of dispersion which can be given by Eq. (3).

$$\sigma_{x0} = R_{11}^2\sigma_{x011} + 2R_{11}R_{12}\sigma_{x012} + R_{12}^2\sigma_{X022}, \tag{3}$$

where $\sigma_{x012} = 0$, and R_{12} should be set as zero to ensure the beam envelope is independent of the initial beam divergence; R_{11}, R_{12} are the elements of the transfer matrix; σ_{x011}, σ_{x012}, σ_{x022} are the elements of initial beam matrix. However, for beams with momentum P_0 and $P_0 + \delta P$, the

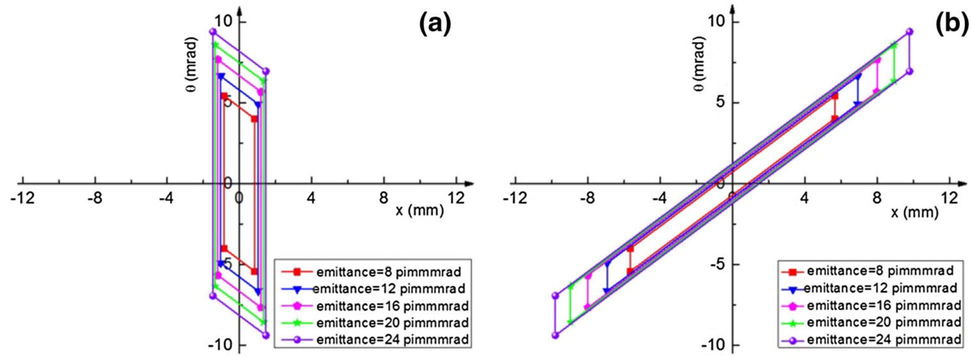

Fig. 3 Phase space: **a** before the entrance collimator, **b** after the exiting collimator (Color figure online)

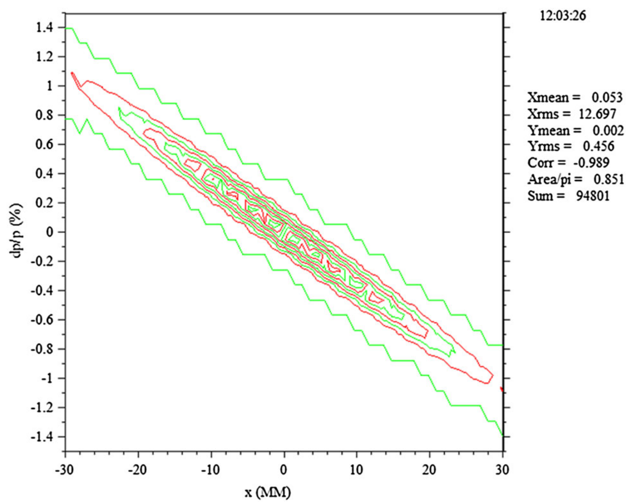

Fig. 4 The correlation between the momentum spread and the horizontal distance (x) to beam axis at slit of the energy selection system. The slope of the ellipse indicates the dispersion R_{16} with -27.54 mm/%. The calculations have been done by the computer code TURTLE [7] and TRANSPORT (Color figure online)

centre distance of such beams can be calculated with Eq. (4).

$$x_\eta = R_{16}\delta. \tag{4}$$

It is obvious that x_η must be more than $2\sqrt{\sigma_{x0}}$ to separate them completely. Therefore, the minimum momentum spread can be obtained by Eq. (5).

$$\frac{\Delta P}{P_{\min}} = \delta_{\min} = \frac{2\sqrt{\sigma_{x0}}}{R_{16}} = \left|\frac{R_{11}}{R_{16}}\right| * 2\sqrt{\sigma_{x011}}. \tag{5}$$

According to the final design, the momentum spread can reach a range about 0.1 to 1% for SC200 ESS, which is equal to the energy spread of about 0.193–1.93% for a proton beam calculated with Eq. (6).

$$\frac{\Delta P}{P} = \frac{E_K + E_0}{E_K + 2E_0}\frac{\Delta E_K}{E_K}, \tag{6}$$

where E_K is the kinetic energy, E_0 is the rest energy of proton, $\Delta E_K/E_K$ is the energy spread, and $\Delta P/P$ is the momentum spread. Eventually, the maximum half-aperture of the slit is set as 28 mm for a maximum of 1% relative beam momentum spread. Meanwhile, all the above elements are aimed at forming a double-bend achromatic system ($R_{16} = R_{26} = 0$) to make the beam transport almost independent of the beam energy.

3 Results and discussion

3.1 Beam optics optimization

Figure 5a shows the beam optics of different initial beams with the same emittance. The result shows that the beam envelopes will decrease when the aperture of the first collimator increases. Table 2 shows the detailed parameters at the slit for different collimation systems, which represent the different initial beam and are calculated based on Eq. (1). It can be seen that the aperture of the second collimator will decrease when the aperture of the first collimator increases. The result also indicates that a smaller aperture will have a higher momentum spread precision. Therefore, it is better to set a smaller aperture after the wedge degrader, which has higher transmission efficiency as shown in Fig. 5b. An important aspect to consider is the location of the maximum beam dimensions and in other words the location for possible beam losses. In the final design of ESS for SC200, the configuration of $R_1 = 1.2$, $R_2 = 8$ is used for an emittance of 16 π mm mrad. The others can be calculated by Eq. (1).

Figure 6a shows the beam optics of different emittances from 8 to 24 π mm mrad with the same Twiss parameter. It is obvious that the beam envelope increases with beam emittance regularity and can be calculated with Eq. (7).

$$u = \varepsilon^{1/2}\beta^{1/2},\ u = x \text{ or } y. \tag{7}$$

This also shows that the dispersion remains unchanged, but the beam size at the slit which increases with the emittance will lead to an enlarging of the minimum momentum spread according to Eq. (3). It can also be seen that the transmission efficiency will increase with the

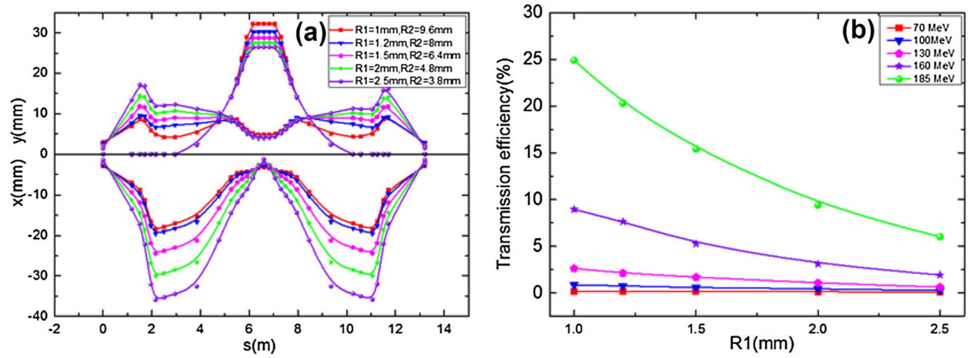

Fig. 5 **a** Beam envelope for a different initial beam with the same emittance, **b** transmission efficiency (Color figure online)

Table 2 Beam parameters at slit of a 0% dispersion beam

Collimation system (mm)	Beam size (mm)	Dispersion (D) (mm/%)	Minimum momentum spread (%)
R_1 = 1, R_2 = 9.6	1.24	− 26.44	0.11
R_1 = 1.2, R_2 = 8	1.58	− 27.54	0.12
R_1 = 1.5, R_2 = 6.4	2.08	− 28.74	0.14
R_1 = 2, R_2 = 4.8	2.79	− 30.27	0.17
R_1 = 2.5, R_2 = 3.8	3.22	− 32.10	0.18

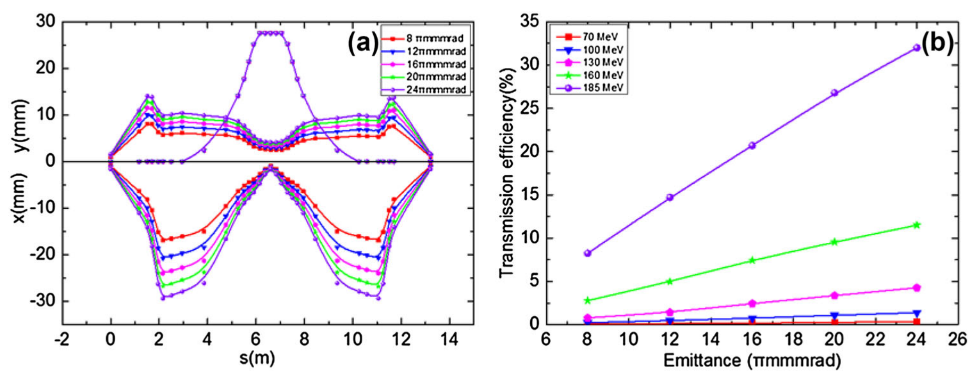

Fig. 6 **a** Beam envelope for different emittance, **b** transmission efficiency (Color figure online)

emittance or energy as shown in Fig. 6b. Therefore, the commission model will be determined by the requirement of beam size, transmission efficiency, and minimum momentum spread during patient treatment. A smaller beam size and higher beam transmission efficiency can be realized with the proton beam of higher energy and lower emittance. That is to say, it will be difficult to have a small beam size and high beam intensity at low energy level.

3.2 Analysis of transmission efficiency

The ESS transmission efficiency has been analysed using a Monte Carlo simulation computer code LISE++ [8], and characteristics of the particle beam should be determined once the initial design is completed and the number of protons tracked is 10^6. In the ESS beamline, there are large beam losses at such points as the degrader, emittance matching, and energy selection as shown in Fig. 7a, b. Therefore, the degrader to the energy slit section will be the most activated region of the ESS beamline. Some local radiation protection calculation (e.g. shielding wall thicknesses, labyrinths, and activations) must be taken into consideration. Figure 7c shows the contribution of the individual components degrader, collimator, and slit system to the loss percentage. The transmission efficiency after the energy slit is strongly dependent on the chosen kinetic energy of the protons, which decreases when the beam energy degrades, and also shows there is almost no beam loss after the slit. As described above, the dose rate of all sources will be determined at relevant locations by assuming certain operating parameters. For example, the most conservative assumption that can be made is as follows: Irradiation shall be given at 70 MeV. Since the cyclotron produces a beam with E = 200 MeV, the beam

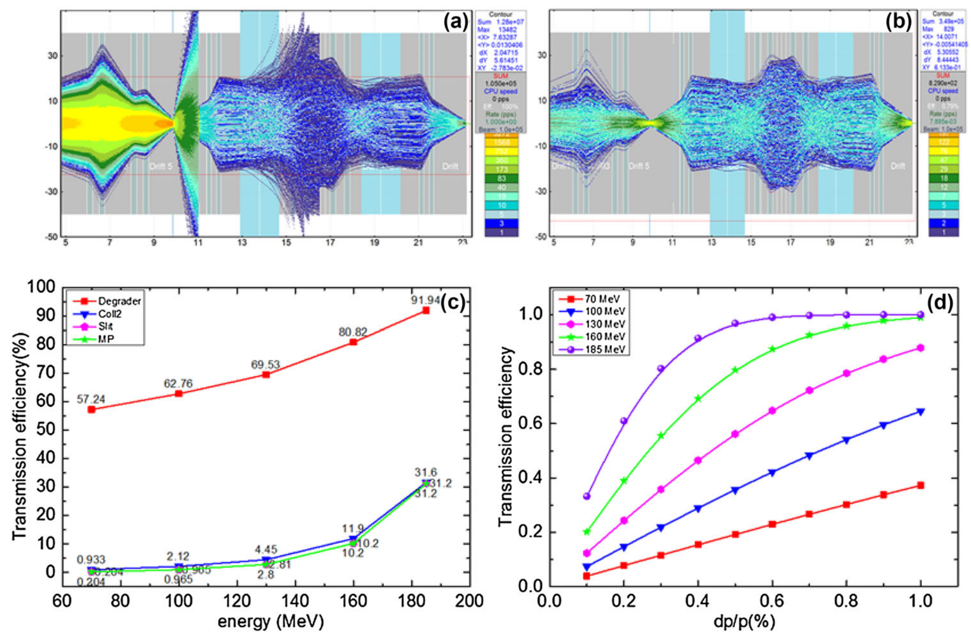

Fig. 7 **a** Beam trajectory for all particles. **b** Beam trajectory only transport through ESS. **c** Transmission efficiency at the degrader, collimator, slit system, and MP. **d** Transmission efficiency for different momentum spread after the slit (Color figure online)

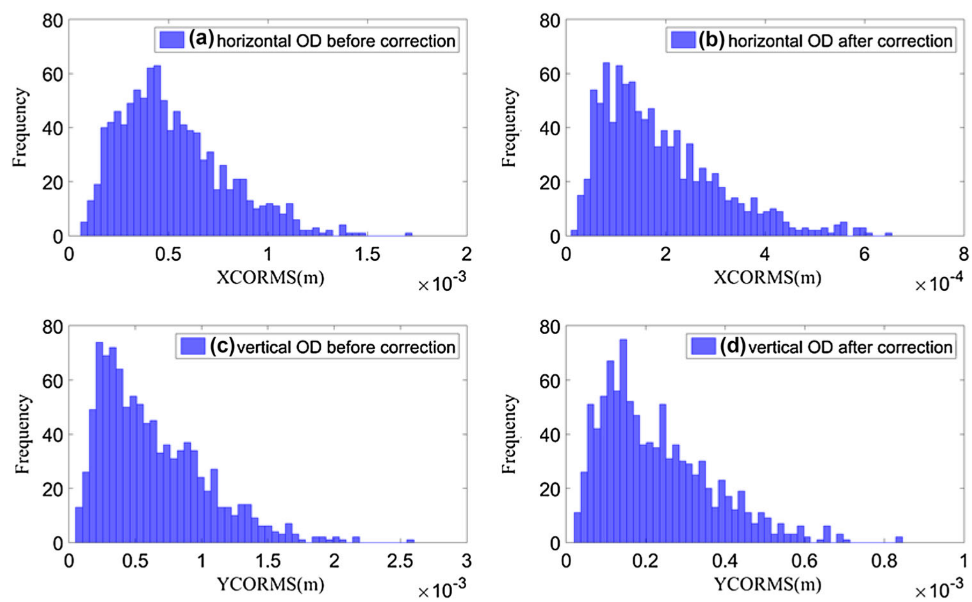

Fig. 8 Excursion distributions of ESS. **a** XCORMS before correction, **b** XCORMS after correction, **c** YCORMS before correction, **d** YCORMS after correction (Color figure online)

must be decelerated in the degrader to 70 MeV. Due to the low transmission at 70 MeV, it needs to be further assumed that the beam current from the cyclotron is at its maximum, that is, up to 500 nA.

An investigation into the transmission efficiency at the slit is introduced in detail. After the degrader, the beam momentum spread distribution for all used energy will obviously be enlarged. A horizontal slit is used to select the required proton and stop others. The relationship between dp/p and the transmission efficiency at the slit is shown in Fig. 7d. Transmission efficiency increases with the momentum spread for a 70–185 MeV proton beam. Consequently, only 0.204% of the beam intensity from the SC200 cyclotron reaches the isocentre of the beam delivery system of the nozzle when proton beams degrade from 200 to 70 MeV, with an acceptance of 24 π mm mrad in each transverse plane and a momentum acceptance of ± 0.6%.

3.3 Orbit distortion correction

Due to the deviations introduced by the magnetic field errors and the misalignments, a series of beam profile monitors for both directions (in x and y) with single steering magnets are used to verify the beam optics and correct the centre trajectory of the proton beam along ESS. In this paper, orbit distortion correction has been calculated

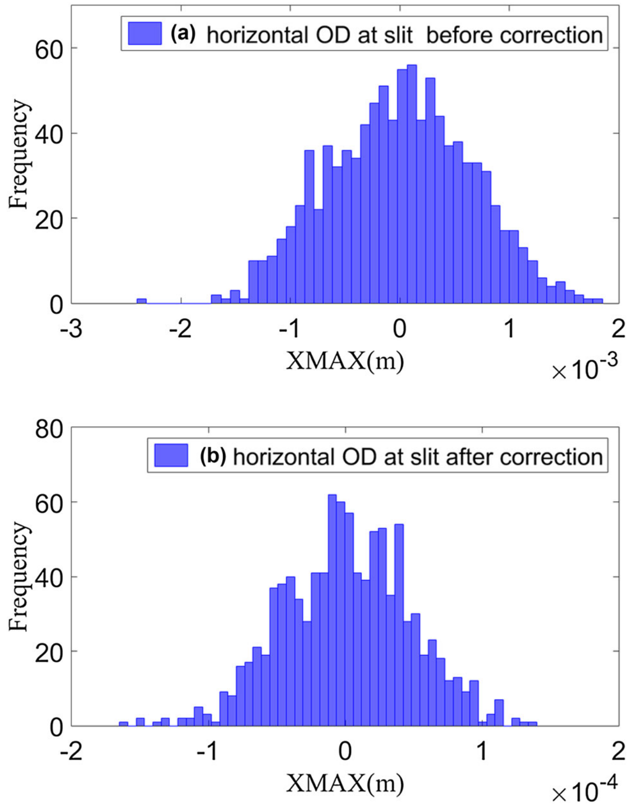

Fig. 9 **a** Excursion distributions at the slit before correction. **b** Excursion distributions at the slit after correction (Color figure online)

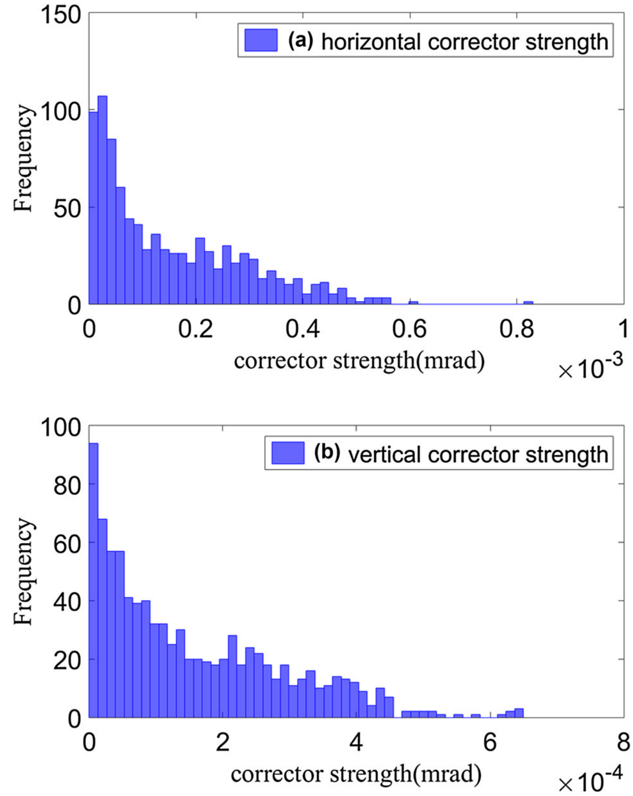

Fig. 10 Maximum absolute corrector strength. **a** Horizontal corrector strength, **b** vertical corrector strength (Color figure online)

with a response matrix and SVD algorithm based on MADX code [9–11]. A statistical analysis simulating 1000 different trajectories with random errors has been carried out before and after the correction. The layout of ESS with six beam position monitors and ten steering magnets is shown in Fig. 2. The position of the beam profile monitors is marked with vertical lines pointing upwards and having labels like BPMn. The positions of the steering magnets required for centring the beam are marked similarly with vertical lines pointing downwards and having labels like Stxn/Styn. The distributions of the RMS orbit distortion (OD) with respect to ESS are evaluated before and after correction as shown in Fig. 8. It is obvious that the beam position at the slit has an extremely high precision after correction as shown in Fig. 9 at about 0.15 mm. Figure 10 shows the distributions of the maximum absolute corrector strength for both horizontal and vertical planes at top energy (E = 200 MeV). On the basis of the error analysis for ESS, the main specifications for steering magnets are summarized in Table 3.

Table 3 Parameters for steering magnets

Parameters	Values
Maximum rigidity (B_ρ)	2.146 T m
Max. deflection angle (θ)	3 mrad
effective length (L_{eff})	0.12 m
Max. magnetic field ($B = \theta/L_{\text{eff}} \times B_\rho$)	536.5 Gs
$\Delta B/BL$	$< 2 \times 10^{-3}$

4 Conclusion

The beam optics of the SC200 ESS beamline has been calculated with the TRANSPORT code on the condition that medical and geometrical constraints have been satisfied. The simulation result indicates that transmission efficiency is extremely sensitive to the initial beam phase space. For beams with the same emittance, a smaller initial beam will be better since it has higher transmission efficiency and smaller minimum momentum spread. For beams with the same Twiss parameters, the beam size, minimum momentum spread and transmission efficiency will increase with emittance. For almost all energies used for proton therapy, analysis of transmission shows that the main factors which influence transmission efficiency of the

SC200 ESS beamline are the degrader, collimator, slit, vacuum system, beam diagnostic system, trajectory and correction system. Moreover, based on statistical analysis of 1000 different simulation trajectories, orbit distortion corrections show that orbit distortion can be corrected to the required precision.

References

1. E. Pedroni, H. Enge, Beam optics design of compact gantry for proton therapy. Med. Biol. Eng. Comput. **33**, 271–277 (1995). https://doi.org/10.1007/bf02510499
2. J.M. Slater, J.O. Archambeau, D.W. Miller et al., The proton treatment center at Loma Linda University Medical Center: rationale for and description of its development. Int. J. Radiat. Oncol. Biol. Phys. **22**, 383–389 (1992). https://doi.org/10.1016/0360-3016(92)90058-P
3. G. Karamysheva,Y. Bi, G. Chen, et al., Compact superconducting cyclotron SC200 for proton therapy, in Proceedings of the 21st International Conference, pp. 371–373 (2016). https://doi.org/10.18429/jacow-cyclotrons2016-thc03
4. M.J. Van Goethem, M.R. Van, H.W. Reist et al., Geant4 simulations of proton beam transport through a carbon or beryllium degrader and following a beamline. Phys. Med. Biol. **54**, 5831–5846 (2009). https://doi.org/10.1088/0031-9155/54/19/011
5. G. Hahn, D.H. An, B.H. Hong et al., A design study of the energy selection system for carbon-ion therapy. J. Korean. Phys. Soc. **66**, 513–517 (2015). https://doi.org/10.3938/jkps.66.513
6. D.C. Carey, K.L. Brown, F. Rothacker, et al., TRANSPORT, A computer program for designing charged particle beam transport systems. SLAC Report No. SLAC-R-95-462
7. D.C. Carey, Turtle: a computer program for simulating charged particle beam transport systems. Fermilab Library Server. 1971
8. O.B. Tarasov, D. Bazin, LISE++: exotic beam production with fragment separators and their design. Nucl. Inst. Methods B **376**, 185–187 (2016). https://doi.org/10.1016/j.nimb.2016.03.021
9. H. Grote, F. Schmidt, Mad-X—an upgrade from mad8, in Proceedings of the Particle Accelerator Conference, 2003. PAC 2003. IEEE, pp. 3497–3499 (2003). https://doi.org/10.1109/pac.2003.1289960
10. C.S.L. Division, W. Herr, S.L. Division, Implementation of new closed orbit correction procedures in the MAD-X program. CERN/SL 2002-2048 (2002)
11. K. Baker, Singular value decomposition tutorial. Ohio State Univ (2005). https://doi.org/10.1021/jo0008901